CIMAC CONGRESS 25
ZURICH, MAY 19 – 23, 2025

2025 | 516

Simulation and optimization of low-pressure power turbine based on supercharged diesel engine.

Turbochargers & Air/Exhaust Management

Yajie Zhang, Shanghai Jiao Tong University

Ling Leng, Shanghai Jiao Tong University
Lei Shi, Shanghai Jiao Tong University

ABSTRACT

Waste heat energy accounts for more than a third of the fuel composition when into engine, thus making WHR technology an important factor in reducing fuel consumption and improving emissions. Turbocompounding is the adition of a power turbine subsequent to the turbocharger turbine and mechanically connected to the engine crankshaft. From a structural and efficiency point of view, the choice of a turbocompounding system is more in line with the needs of diesel supercharged engine optimization.

Based on experimental data from a supercharged diesel engine bench at the New Energy Power Research Institute of Shanghai Jiao Tong University, a modification scheme for the power turbine is proposed for low pressure ratio and small flow rate conditions. A 3-D model of the turbine is established using inverse design, and a 3-D steady-state model is built by means of Computational Fluid Dynamics (CFD) to analyse and calculate the working state of the turbine under the target operating conditions. The optimization direction is confirmed under the guidance of the 1-D model of the turbine operating principle. The training set is constructed using the LHS sampling method, and the optimization scheme is determined by neural networks and genetic algorithms to obtain the structural parameters of the power turbine suitable for the operating conditions. The analysis and calculation results prove that the optimization scheme can effectively reduce the internal flow loss of the turbine, improve the flow situation and increase the efficiency.

1 INTRODUCTION

Turbocompound technology adds a low-pressure power turbine (LPT) after the turbocharger turbine aim at recover exhaust gas energy, improve engine thermal efficiency, reduce BSFC (Brake Specific Fuel Consumption) and enhance the engine's environmental suitability. The power turbine is able to operate independently of engine speed and supercharger speed, increasing freedom of control.

Exhaust temperature and supercharger speed are important limiting factors for turbochargers at plateau conditions [1], while altitude significantly affects the available exhaust energy and the optimal energy distribution among multiple turbines. By studying the turbocharger regulation law at different altitudes, the performance of turbocharged engines can be improved in a wide range of altitudes, Zhao [2] analysed the influence of different components in the composite turbocharging system on fuel consumption through simulation models. As illustrated in Figure 1, a reduction in pressure at the outlet of the power turbine is conducive to a decrease in fuel consumption of the composite turbocharged engine, thereby providing additional power output to reduce fuel consumption of the composite turbocharged engine.

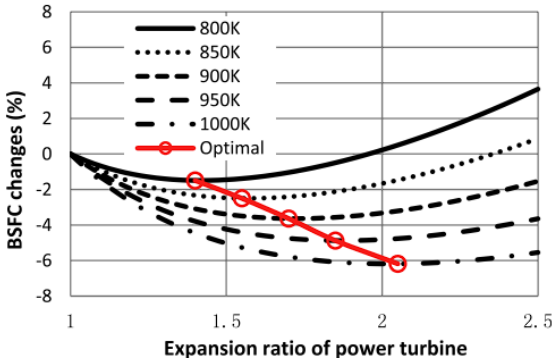

Figure 1. The impacts of exhaust temperature on BSFC changes and optimal power turbine expansion ratio

The power turbines frequently work in conditions of low expansion ratio (less than 1.3) due to the presence of high exhaust pressure in the exhaust manifold [3] and deviating from the design operating point with low energy recovery. The lack of efficiency prediction models for low expansion ratio power turbines means it is difficult to design a power turbine for a specific exhaust energy recovery scenario. The paper builds a performance prediction model of low-expansion-ratio power turbines based on 3D simulation. data; proposes a structural optimisation scheme based on the model to improve the exhaust energy recovery efficiency; and compares the performance profiles of the prototype and optimised turbine to prove the optimal design of the power turbine structure on the composite turbine engine performance improvement.

2 CFD（COMPUTATIONAL FLUID DYNAMICS） SIMULATION OF LOW-PRESSURE POWER TURBINE

A turbocompound dynamics model based on the modified SC7H245Q5 diesel engine of Shanghai Diesel Engine Co. Ltd. is selected for the study of the power turbine therein. The model of the power turbine is Garrett GT4082, which has a low expansion ratio due to high exhaust backpressure. The operational limitations of the generator, with an operational speed below 22000r/min, result in deviations from the turbine's designed operational conditions, thus significantly reducing its efficiency.

(a) Turbocompound diesel engine test bench
(b) Turbocompound system structure
Figure 2. Turbocompound diesel engine performance and emission test bench

CFD can accurately simulate inner phenomena of turbine's complex flow and predict turbine performance, still, the computational cost is too high. In this section, the numerical simulation model of LPT is firstly calibrated based on experimental data. Subsequently, the sensitivity analysis of individual geometric parameters to the total-static efficiency of LPT. Following this, the influence of single geometric parameters and the range of optimised values is determined, after which the optimised geometric parameters and of the parameters are obtained. Then, the relationship model between the geometric parameters and the LPT's total-static efficiency is established using a backpropagation (BP) neural network. Through the genetic algorithm (GA) of local searching for the optimum, new geometric parameters are obtained. New geometric parameters are obtained; finally, a comparison is made of the turbine performance between former and optimised model, and evaluate the turbine performance prediction model and optimisation scheme.

2.1 Inverse Design of Turbine Model

Scanning and measuring the GT40 turbine physical object to construct a 3D model, and reverse design

analysis in CFturbo22.4 to obtain the meanline model. The key geometric parameters of the GT40 turbine are shown in Table 1, and the meanline model of the turbine is shown in Figure 3. The 3D model of the turbine is shown in Figure 4. In order to prevent backflow, it is necessary to extend the inlet and outlet tubes by a factor of five their respective diameters.

Table 1. Key geometric parameters of GT40 turbine

geometric parameter	Value
Impeller parameters	
Rotor diameter(mm)	78.556
Inlet width(mm)	12.678
Blade angle inlet (°)	2.4
Outlet hub diameter(mm)	22.75
Outlet shroud diameter(mm)	70.89
Blade angle outlet (°)	-37.7
Number of Blades	10
Volute parameters	
Center line diameter(mm)	80
Mean Radial Height	130

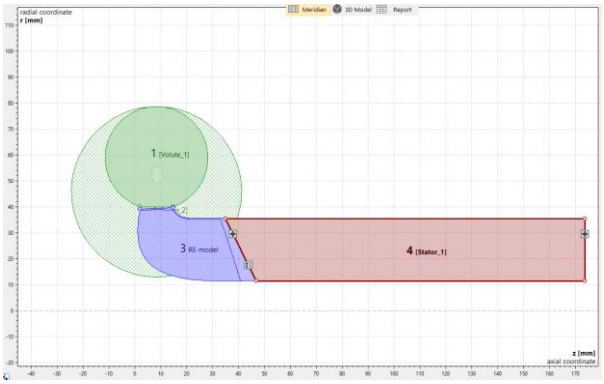

Figure 3. Meridional plane model in CFturbo2022.2.4

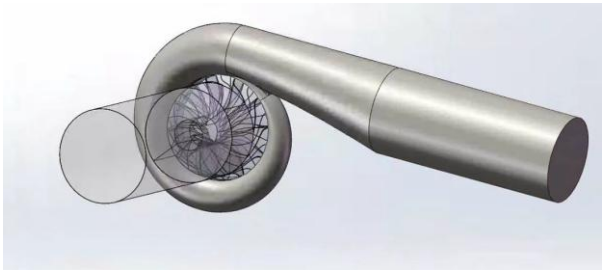

Figure 4. 3D model in SOLIDWORKS

2.2 Establishment of CFD coupled simulation model in Workbench

The CFD coupled simulation model of the turbine is established in the commercial software ANSYS Workbench. The single flow passage model is transferred from CFturbo through batch to transfer relevant parameters, then the impeller data are transferred to TurboGrid to generate the structured mesh of turbine impellers and turbine outlet pipe, and then transferred to CFX module to set the boundary conditions and the working environment, and then carry out the iterative calculations.

The impeller tip clearance is taken as 0.3 mm.The interface between the rotating and stationary domains is considered as 'frozen rotor' in steady case and as 'transient rotor-stator' in unsteady case. For steady state, total inlet pressure and total temperature are used as inlet boundary conditions and outlet static pressure as the outlet boundary condition. The wall surface is assumed to be adiabatic without slip, and the wall function method is used in the near-wall region. The medium inside the GT40 turbine is a gas, considered as an incompressible ideal gas, and the governing equations are the continuity equation (conservation of mass), momentum equation (conservation of momentum) and energy equation (conservation of energy). The full development of turbulence in the turbine flow field and the boundary layer in the near-wall region are simulated by k-omega SST. Empirical equation for turbulence intensity (Eq.1) indicates that the turbulence intensity of the model is 0.01.

$$I = \frac{u'}{U} = 0.16(\mathrm{Re}_{DH})^{-\frac{1}{8}} \quad (1)$$

where, Re_{DH} - equivalent diameter Reynolds number,U- average turbulent velocity.

TurboGrid generated a structured mesh with a mesh growth rate of 1.3, while the height of the first layer of the near-wall mesh is 5e-6 m. The non-structured mesh of volute is generated in Mesh, considering the influence of the boundary layer on the solid-wall face of volute, with the first layer of the mesh-4e-5 m, where a growth rate of mesh is 1.2, with a maximum of 5 layers of boundary layer.

However, it is not sufficient to obtain accurate solutions once a certain density has been reached. For the RANS model, it has been demonstrated that increasing the mesh density will not result in a more accurate solution once the mesh has reached a certain density.

As illustrated in Table 2, the mesh size of single-passage impeller is selected to be 85w, and the mesh size of volute is 280.9w. The boundary conditions are set in accordance with the design conditions, when the flow rate is 0.1124 kg/s and the total-static efficiency is 66%. As demonstrated in Table 2, when the number of grids is set at 850320, the relative error is less than 1%, the relative error of the flow rate with the test value is

3.1%, and the relative error of the total - static efficiency with the test value is 2.0%.

Table 2. Independence analysis of mesh size

Mesh size	Mass flow(kg/s)	Relative error (%)	Total-static efficiency (%)	Relative error (%)
533325	0.11579		77.23	
643003	0.115949	0.13	64.10	17.00
740202	0.11594	-0.01	64.86	1.18
850320	0.115884	-0.04	64.71	0.23
1075648	0.115812	-0.06	64.73	0.04
1260792	0.115858	0.04	64.71	-0.04
1590232	0.115837	-0.02	64.73	0.03

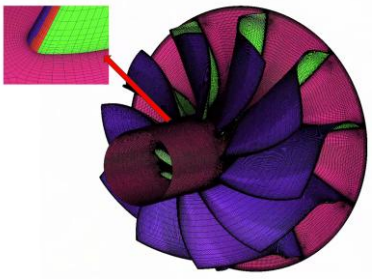

(a) Structured mesh in impeller

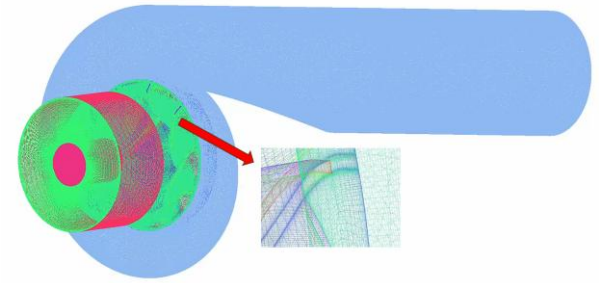

(b) Full view of mesh in turbine

Figure 5. Turbine mesh generation

3 ESTABLISHMENT OF LPT PERFORMANCE PREDICTION MODEL

In this section, the sensitivity between turbine geometric parameters and total-static efficiency is firstly analysed. The selected geometric parameters are then used to create a training set by LHS (Latin Hypercube Sampling) method, and the efficiency prediction model is obtained by training using BP neural network.

As Figure 6 shows the work process of the turbine, two assumptions are involved in approximate calculations of efficiency in radial turbines: the gas is adiabatic throughout the work process, i.e., the adiabatic index γ is kept constant; the state of the gas inside the turbine is described using a mean value model.

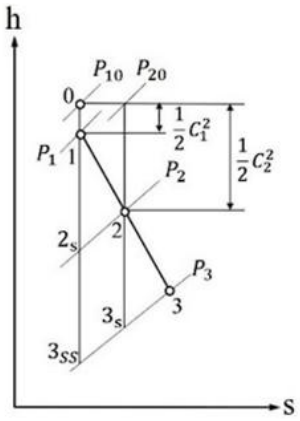

Figure 6. Enthalpy-entropy diagram of turbine work process

The total-static and total-total efficiencies of the radial turbine are calculated according to Eq.2 and 3. LPT describes the efficiency of doing work in terms of total-static efficiency.

$$\eta_{ts,T} = \frac{T_{02} - T_{03}}{T_{01} - T_{3s}} = \frac{1-(T_{03}/T_{02})}{1-(P_3/P_{01})^{(\gamma-1)/\gamma}} \quad (2)$$

$$\eta_{tt,T} = \frac{T_{02} - T_{03}}{T_{01} - T_{03s}} = \frac{1-(T_{03}/T_{02})}{1-(P_{03}/P_{01})^{(\gamma-1)/\gamma}} \quad (3)$$

The thermocouple in the test system measures the static temperature and pressure, then the total temperature and pressure are calculated using Eq.4,5 and 6.

$$T_0 = (1+\frac{k-1}{2}Ma^2)\cdot T \quad (4)$$

$$P_0 = (1+\frac{k-1}{2}Ma^2)^{k/k-1}\cdot P \quad (5)$$

$$Ma = \frac{\dot{m}/\rho A}{\sqrt{kRT}} \quad (6)$$

As in Figure 7, the impeller inlet and outlet velocity triangles are defined by the following equations: 7, (a) and (b) are the impeller inlet and outlet velocity triangles.

where C-absolute velocity, U-circumferential velocity, W-relative velocity, C_θ-circumferential component velocity of the absolute velocity, W_θ-circumferential component velocity of relative velocity, C_r and C_a-radial and axial velocities, α-absolute airflow angle, β-relative airflow angle, and

subscript 2-inlet of impeller, subscript 3-outlet of impeller. The velocity triangle can be solved through the combination of mass conservation equations for each control surface and the turbine's geometric parameters.

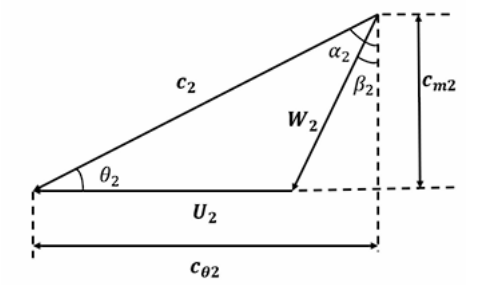

(a) Inlet velocity triangle of turbine

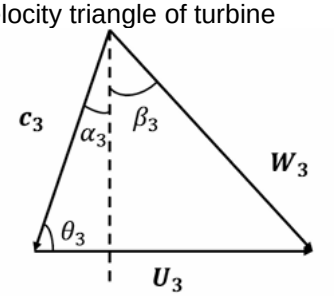

(b) Outlet velocity triangle of turbine

Figure 7. Velocity triangle of turbine

Moreover, according to Euler's equation, the actual work of the turbine can be calculated directly from the velocity triangle (Eq.7).

$$\frac{W_{act}}{\dot{m}} = U_2 C_{\theta 2} - U_3 C_{\theta 3} = \frac{1}{2}\left[\left(U_2^2 - U_3^2\right) + \left(W_2^2 - W_3^2\right) - \left(C_2^2 - C_3^2\right)\right] \quad (7)$$

Consequently, changing the geometric parameters of the turbine inlet and outlet will affect the turbine's efficiency in performing work, and models exist that can express this relationship.

3.1 Sensitivity analysis of geometric parameters

3.1.1 Inlet geometry parameters of LPT

Both the rotor diameter and the inlet width affect the magnitude of the flow into the turbine and influence the inlet angle of attack to affect the internal flow and efficiency of the LPT. The boundary conditions remain constant, with a single variable being altered for CFD calculations.

When the mass flow rate through the turbine is constant, altering the rotor diameter, either by increasing or decreasing it, results in a corresponding alteration of the flow rate. The flow rate is associated with flow loss; when the flow rate is overly high, it can lead to boundary layer separation, an increase in turbulent losses, and a subsequent decrease in efficiency. As shown in Figure 8, increasing the rotor diameter from 71 mm results in an initial increase in LPT efficiency, followed by a subsequent decrease. The maximum efficiency ranges between 78 and 79 mm.

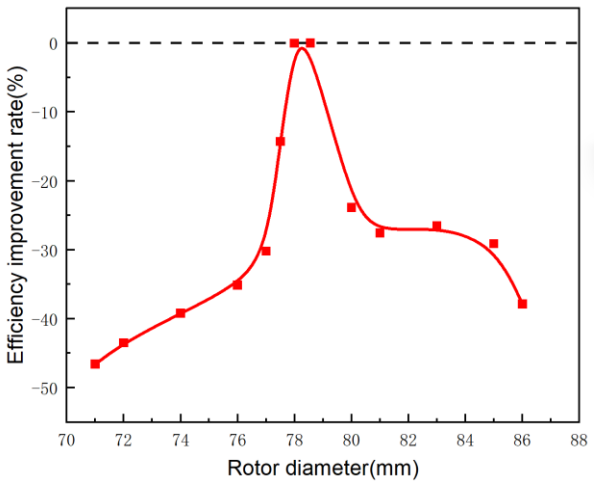

Figure 8. Effect of rotor diameter on LPT's efficiency

When the mass flow rate through the turbine is constant and the inlet width is modified, the efficiency of LPT increases initially with the impeller inlet width and subsequently stabilises, as illustrated in Figure 9. It is demonstrated that an augmentation in the inlet blade width can enhance flow characteristics, thereby reducing angle-of-attack loss and vortex loss. However, it is noteworthy that an excessively wide inlet width may precipitate backflow.

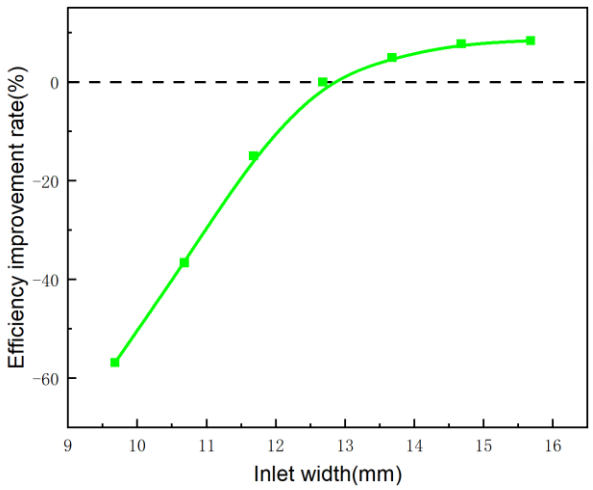

Figure 9. Effect of inlet width on LPT's efficiency

3.1.2 Outlet geometry parameters of LPT

As Fig. 10 illustrates, the boundary conditions remain constant. The LPT efficiency initially rises before decreasing as the outlet hub diameter increases. When the outlet hub diameter is excessively small, flow loss is exacerbated due to the outlet being too diminutive. In contrast, when the outlet hub diameter is overly large, backflow occurs. Therefore, the suitable range of values for the hub is 22.5-24.5 mm.

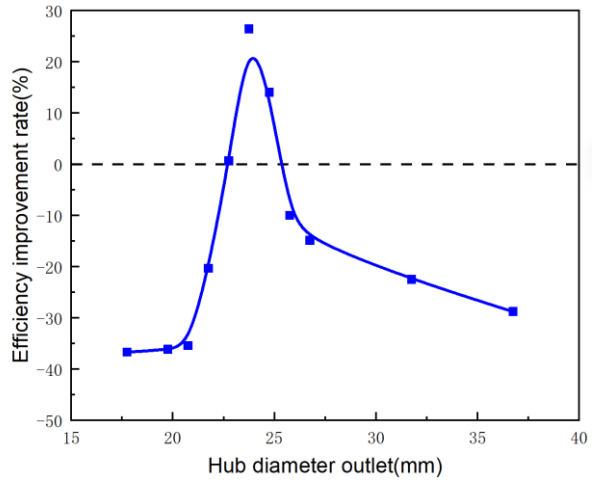

Figure 10. Effect of outlet hub diameter on LPT's efficiency

As shown in Figure 11, the turbine efficiency is observed to decrease and then increase as the turbine outlet centreline diameter increases. Excessively small blade outlet centreline diameters can result in clogging, whereas excessively large centreline diameters can lead to backflow with a substantial negative pressure gradient. Consequently, this value should be constrained in consideration of the design requirements. Compared to other geometrical parameters, the effect of outlet midline diameter on LPT efficiency is minor, less than 10%.

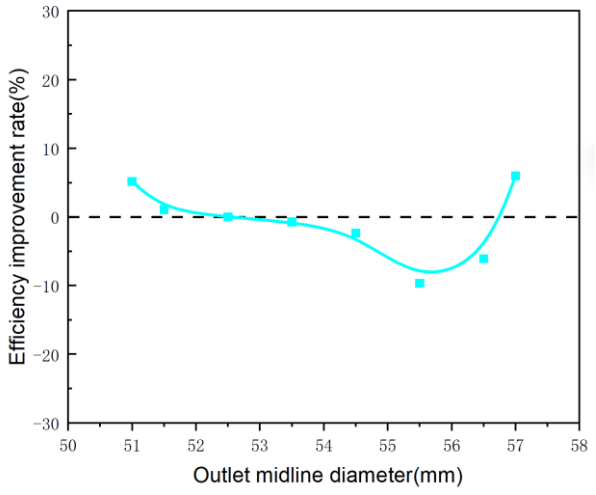

Figure 11. Effect of outlet shroud diameter on LPT's efficiency

3.1.3 Blade length

With the increase of blade length, the LPT efficiency increases firstly and then decreases with the increase of blade length. Increases in blade length have given rise to the hypothesis that the medium is able to perform its function in the turbine to a greater extent. This is because the pressure gradient becomes smaller, resulting in a reduction of leakage at the tip of the blade and suppression of secondary flow. However, excessive blade length leads to friction loss, which in turn causes deterioration of the load distribution on the blade surface and reduction of efficiency. Therefore, appropriate limits must be established.

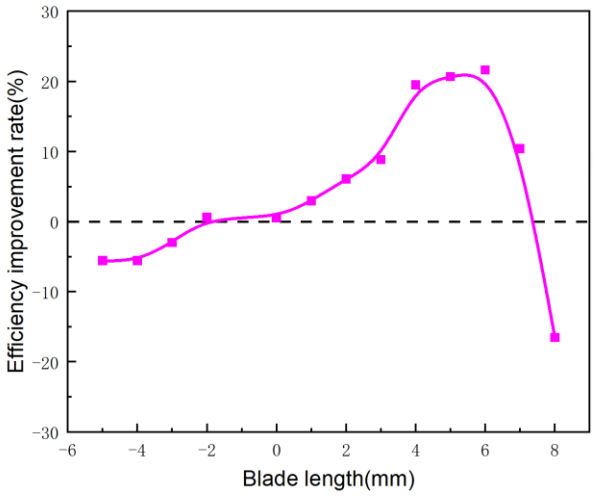

Figure 12. Effect of blade length on LPT's efficiency

Through analyse of geometric parameters, outlet hub diameter, outlet shroud diameter, and blade length have been set as primary contributors to LPT efficiency. In the following section, these parameters will be utilised as training set to develop a prediction model for LPT efficiency.

3.2 LPT efficiency prediction model based on geometric parameters

3.2.1 LHS sampling to construct the training set

A geometric parameter space consisting of outlet hub diameter, outlet shroud diameter and blade length was constructed using LHS sampling to calculate the LPT efficiency of the turbine based on 3D for different combinations of geometric parameters. The sampling intervals for the geometric parameters are illustrated in Table 3, with 100 sampling points (Figure 13).

Table 3. LHS sampling range for geometric parameters of impeller

Outlet hub diameter(mm)	Outlet shroud diameter	Blade length-axial extension in meridional plane(mm)
[15,35]	[58,78]	[24.587,40.587]

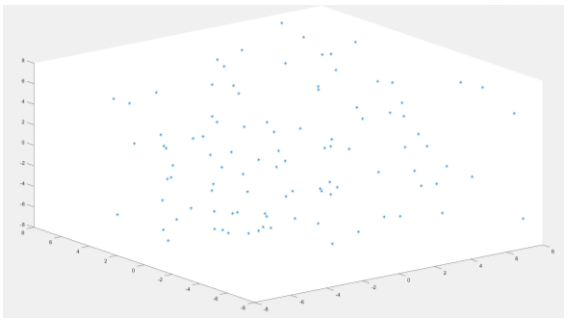

Figure 13. Spatial distribution of LHS sampling point

3.2.2 BP (Back Propagation) Neural Network Training

The relationship between geometric parameters and LPT efficiency is complex and difficult to describe, yet it can be modelled using BP neural network. The training set, obtained by the LHS method, is randomly divided into training, testing and validation sets in the following proportions: 70%, 15%, 15%. Choose Sigmoid for activation function. The training method for this process was selected as Levenberg-Marquardt for supervised learning.

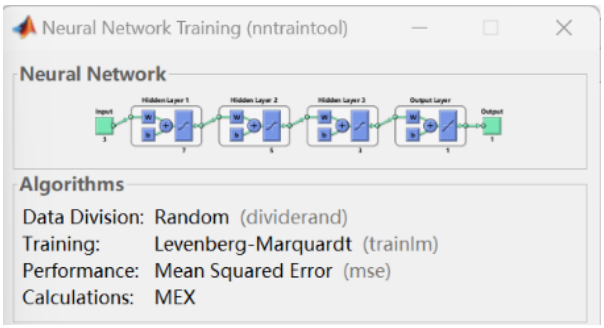

Figure 14. BP neural network architecture

Mean Square Error was designated as the training error. The number of hidden layers of the neural network is 1, and according to the empirical formula Eq. 8, the number of hidden neurons is selected as 3.

$$n_1 = \sqrt{(n_2 + m_2)} + a_2 \qquad (8)$$

where n_2 and m_2 are the number of neurons in the input and output layers, respectively, and a_2 is an empirical constant, usually in the range 1-10.

R2 and RMSE (Root Mean Square Error) are utilised to evaluate the predictive capability of the model.RMSE is utilised as a metric to quantify the discrepancy between the predicted and measured values of the model. The lower the value of RMSE, the more the predicted values match with the actual values, and the higher the accuracy of the model prediction.

$$R^2 = \frac{\left(n\sum_{i=1}^{n}x_i y_i - \sum_{i=1}^{n}x_i \cdot \sum_{i=1}^{n}y_i\right)^2}{\left(n\sum_{i=1}^{n}x_i^2 - \left(\sum_{i=1}^{n}x_i\right)^2\right)\cdot\left(n\sum_{i=1}^{n}y_i^2 - \left(\sum_{i=1}^{n}y_i\right)^2\right)} \qquad (9)$$

$$RMSE = \sqrt{\frac{1}{n}\sum_{i=1}^{n}\left(x_i' - x_i\right)^2} \qquad (10)$$

According to the calculation, each error is minimised when the number of hidden neurons is 3.

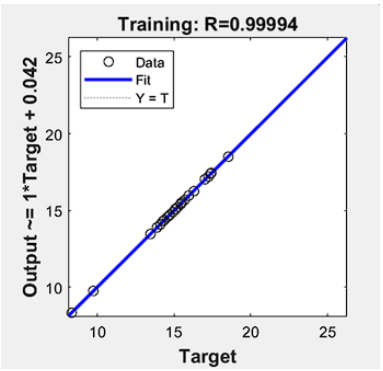

Figure 15. R-squared value of BP neural network predicting LPT efficiency

4 LPT STRUCTURE OPTIMISATION

4.1 GA optimization settings

Since the optimisation parameters are numerous, discrete and highly non-linear, a genetic algorithm is applied to calculate the local optimum with the parameters set as in Table 4.

Table 4. Parameter settings of GA optimization algorithm

Parameter	Value
Population size	100
Population type	Double vector
Scaling function	Proportional

Selected function	Tournament
Tournament size	4
Crossover fraction	0.8
Mutation rate	0.01
Migration direction	Both
Migration fraction	0.2

The fitness function is based on the LPT efficiency prediction model construction constructed in 3.2.2 Construction

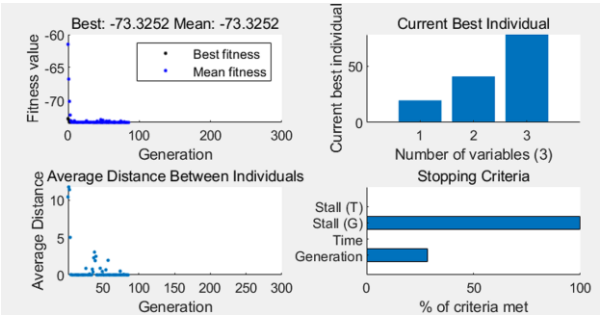

Figure 16. GA algorithm optimisation results in matlab

The geometrical parameters of the impeller before and after optimisation are shown in Table 5. The optimised outlet hub diameter and blade length are significantly increased, and the impeller inlet diameter is slightly reduced.

Table 5. Comparison of key geometric parameters of impeller between original and optimised values

Geometric parameter	Original value	Optimised value
Rotor diameter(mm)	78.556	78
Outlet hub diameter(mm)	22.75	27.376
Outlet shroud diameter(mm)	70.89	70.89
Blade length-axial extension in meridional plane(mm)	32.587	39.868

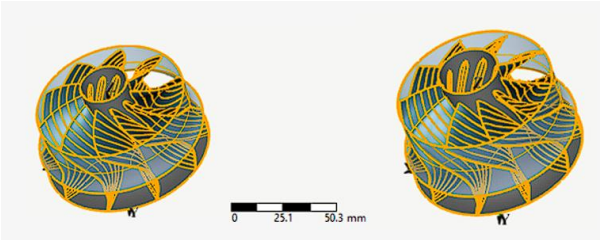

(a) Original model
(b) Optimised model

Figure 17. GA algorithm optimisation results in matlab

The total-static efficiency of the optimised LPT is **76.5%**, which is 15.9% higher than the total-static efficiency of the original LPT. This result meets the design objective of high efficiency recovery under low expansion ratio operating conditions.

4.2 Analysis of optimisation results

Post-processing and result analysis of CFD-based calculation of LPT performance can be carried out by targeting impeller blade height sections and chord length sections at different locations. This approach facilitates the investigation of the impeller geometry's impact on performance and the analysis of key factors influencing the efficiency performance index. Concomitantly, it is imperative to comprehend the flow phenomena, such as separation and vortex of flow inside the impeller, identify the primary sources of flow loss, in case to provide guidance for optimal design.

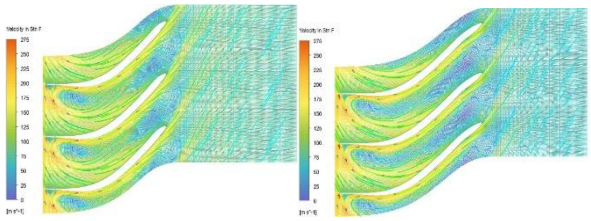

Figure 18. Absolute velocity distribution in the impeller passage (at 80% span)

As Figure 18 illustrates, the distribution of absolute velocity is observed at 80% span within the impeller passage. Upon optimisation, the absolute velocity at the outlet is apparently reduced, the absolute Mach number at the outlet is decreased, and the flow expands more fully inside the impeller. Under constant mass flow rate conditions, the pressure drop is increased and the actual work of the turbine is elevated. The change in absolute velocity at the impeller outlet corresponds to the change in residual velocity loss.

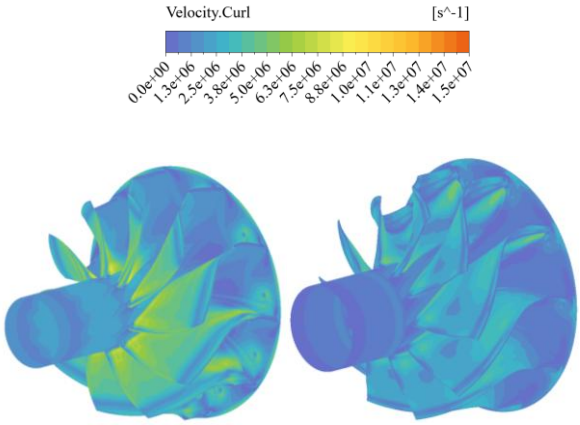

(a) Original model
(b) Optimised model

Figure 19. Vorticity distribution contour plots in whole passages

The flow loss control mechanism that affects the efficiency of the LPT is analysed using vortex contour plots. The region of high vorticity in the leading edge surface of the blade is concentrated in the suction surface and tip region. Because the impeller is designed to have a negative angle of incidence over the leading edge span, local vorticity is created near the suction surface at the leading edge of the impeller. Near the tip of the blade, the flow continues to move towards the pressure surface due to the local vorticity created by the relative motion between the tip of the blade and the casing, while at the pressure surface the vorticity created by the leakage from the tip of the blade remains in the centre of the channel near the tip of the blade. Comparing the vortex distribution at different blade chord length positions along the flow direction before and after optimisation, the vortex near the suction surface is smaller after optimisation at the leading edge of the blade; in the middle and rear sections of the blade, especially at the trailing edge of the blade, the high vortex region is significantly reduced after optimisation, the secondary flow is weakened, and the vortex generated by the leakage from the tip of the impeller tip is significantly reduced due to the lengthening of the blade.

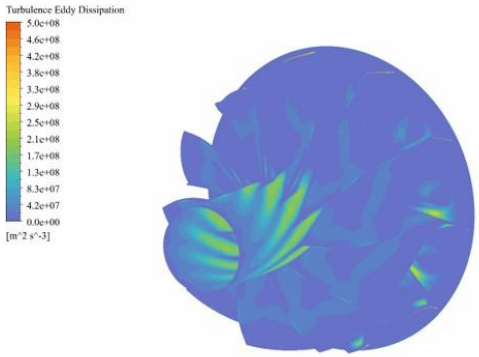

(a) Original model

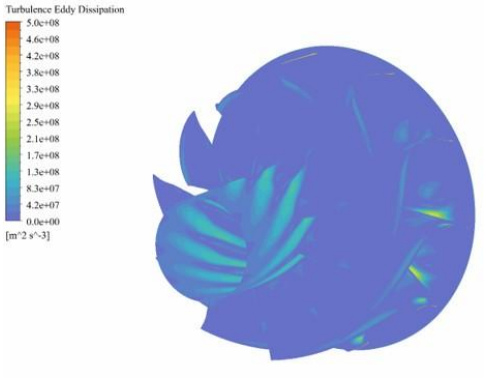

(b) Optimised model

Figure 20. Turbulence dissipation contour plot

The turbulent dissipation rate is defined as the energy loss due to the viscous and turbulent motion of the fluid. Figure 20 illustrates the turbulent dissipation rate distribution. The turbulent viscous dissipation near the trailing edge of the impeller and at the outlet of the impeller passage is significantly reduced compared to the origin turbine. This suggests that the optimised LPT has less energy loss in the impeller passage and is more efficient in doing work.

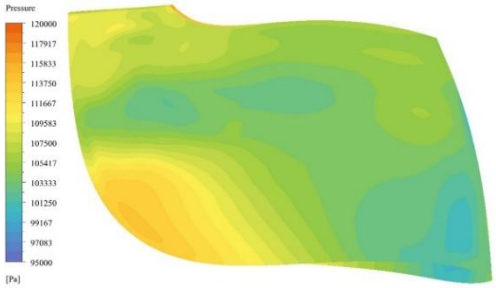

(a) Pressure side-original

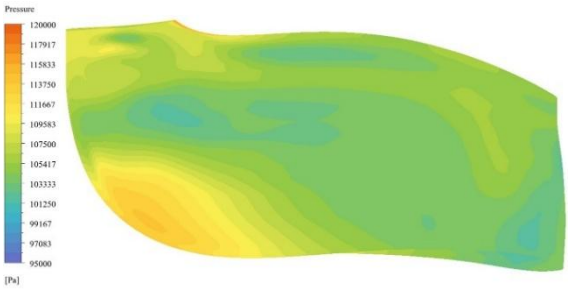

(b) Pressure side-optimised

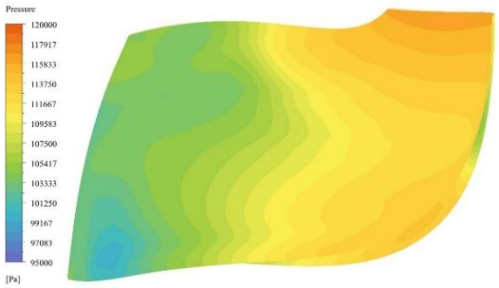

(c) Suction side-original

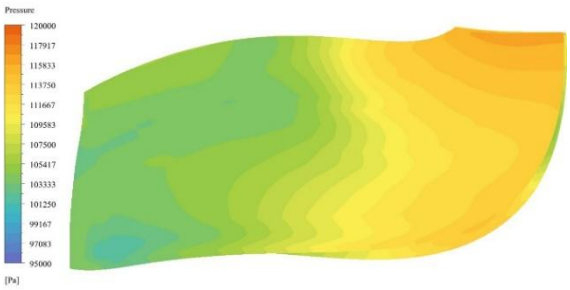

(d) Suction side-optimised

Figure 21. Blade loading at pressure side and suction side

The preceding analysis demonstrates that the blade extension design enhances turbine efficiency under the specified conditions, predominantly by augmenting the degree of expansion of the flow within the impeller, thereby minimising impeller secondary flow loss and tip leakage loss. Concurrently, residual velocity loss remains relatively constant despite fluctuations in outlet cyclone intensity. The optimised design of LPT enhances the performance by integrating the effects of multiple loss factors.

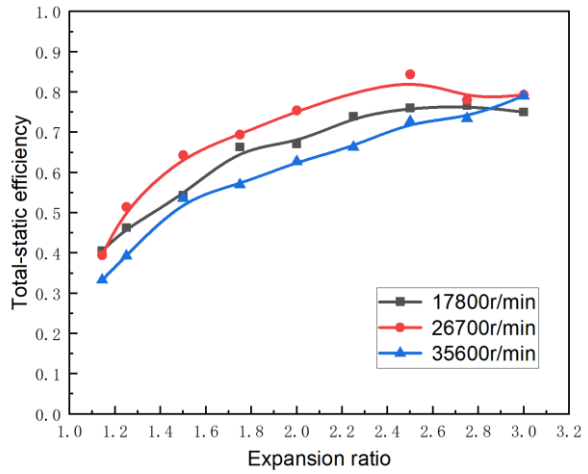

(a) Original model

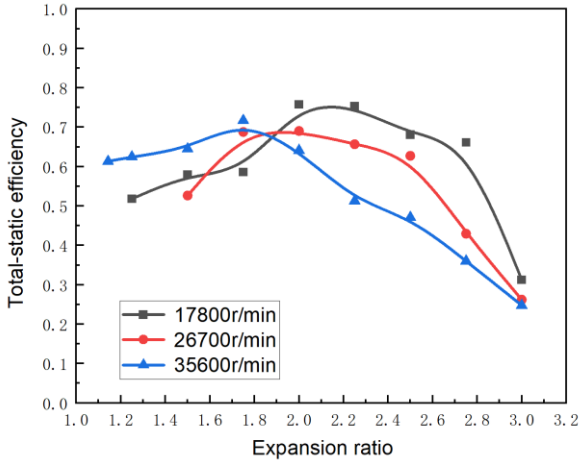

(b) Optimised model

Figure 22. Turbine's efficiency MAP origin and optimised

By comparing the efficiency curves within the working speed of the LPT, the optimised turbine is more efficient in low expansion ratio region, and its performance is comparable to that of the original model at medium expansion ratio region. However, the poor efficiency of the optimised model in high expansion ratio region could be attributed to the fact that the reduction of the flow loss caused by the extend length of the blades is larger than the work done by the expansion. Overall, the LPT obtained by the design is able to satisfy the design requirements.

5 CONCLUSIONS

(1) The physical inverse design for the reconstruction of the turbine model, in conjunction with 3D simulation calculation of the power turbine, provides a foundation for subsequent research. Compared against the experiment data, the mass flow error and the total - static efficiency error at the design point is less than 5%, which can be used as a basis for subsequent research.

(2) The present study investigates the influence pattern of the turbine key geometric parameters on the total-static efficiency of LPT, and the geometric parameters that have a greater influence on the efficiency are screened out. Establishing a machine learning-based LPT efficiency prediction model is undertaken, with the incorporation of GA for structure optimisation. The optimisation process has been streamlined, and the predictive model is extensible.

(3) The optimisation results are analysed to study the loss mechanism inside the LPT impeller. An increase in blade length, enabling adequate function of the gas, enhances efficiency and reduces flow loss under low expansion ratio conditions. However, this enhancement disappears or worsens as the expansion ratio rises. The performance of the optimised turbine is verified to meet the design requirements, and it is proved that the design scheme can be applied to the power turbine in low and medium expansion ratio conditions.

6 REFERENCES AND BIBLIOGRAPHY

[1] Yang M, Gu Y, Deng K, et al.2018.Influence of altitude on two-stage turbocharging system in a heavy-duty diesel engine based on analysis of available flow energy, *Applied Thermal Engineering*,129:12-21

[2] Zhao R,Zhuge W,Zhang Y,et al. 2016.Parametric study of a turbocompound diesel engine based on an analytical model,*Energy*,115(1):435-445

[3] Kapich, D., "Turbo-Hydraulic Engine Exhaust Power Recovery System," SAE Powertrain & Fluid Systems Conference & Exhibition, San Diego, USA, 2002.

7 CONTACT

Zhang Yajie

zyjchocolate@sjtu.edu.cn